

## Level statistics for quantum $k$ -core percolation

L. Cao and J. M. Schwarz

*Physics Department, Syracuse University, Syracuse, New York 13244, USA*

(Received 22 March 2012; published 24 August 2012)

Quantum  $k$ -core percolation is the study of quantum transport on  $k$ -core percolation clusters where each occupied bond must have at least  $k$  occupied neighboring bonds. As the bond occupation probability  $p$  is increased from zero to unity, the system undergoes a transition from an insulating phase to a metallic phase. When the length scale for the disorder  $l_d$  is much greater than the coherence length  $l_c$ , earlier analytical calculations of quantum conduction on the Bethe lattice demonstrated that for  $k = 3$  the metal-insulator transition (MIT) is discontinuous, suggesting a new type of disorder-driven quantum MITs. Here, we numerically compute the level spacing distribution as a function of bond occupation probability  $p$  and system size on a Bethe-like lattice. The level spacing analysis suggests that for  $k = 0$ ,  $p_q$ , the quantum percolation critical probability, is greater than  $p_c$ , the geometrical percolation critical probability, and the transition is continuous. In contrast, for  $k = 3$ ,  $p_q = p_c$ , and the transition is discontinuous such that these numerical findings are consistent with our previous work to reiterate a new random first-order phase transition and therefore a new universality class of disorder-driven quantum MITs.

DOI: [10.1103/PhysRevB.86.064206](https://doi.org/10.1103/PhysRevB.86.064206)

PACS number(s): 71.23.An, 72.15.Rn, 71.30.+h

### I. INTRODUCTION

With the exception of transition-metal compounds, there exist two conventional paradigms for metal-insulator transitions (MITs): a Mott-Hubbard-type transition and an Anderson-type transition. The former is a consequence of tuning the interactions between electrons by changing the distance between atoms, for instance, and the MIT is discontinuous.<sup>1</sup> The latter is a consequence of tuning the disorder in the material, and the MIT is continuous.<sup>2,3</sup> Recently, a discontinuous disorder-driven MIT has been predicted for a model in which there exists geometric constraints on the disorder.<sup>4</sup> The model has been dubbed quantum  $k$ -core percolation. Quantum  $k = 0$  core percolation, or quantum percolation (QP), has been studied since the 1980s and exhibits a continuous, Anderson-type MIT.<sup>5,6</sup> Quantum percolation is defined accordingly. Consider a lattice whose bonds are occupied independently and at random with bond occupation probability  $p$ . An electron can only hop between lattice sites  $i$  and  $j$  along an occupied bond and cannot hop along an unoccupied bond. In addition, there exists a constant on-site binding energy which is set to zero for convenience. In total, the tight-binding Hamiltonian for quantum percolation is

$$H = \sum_{i,j} t_{ij} a_i^\dagger a_j + \text{H.c.}, \quad (1)$$

in which

$$t_{ij} = \begin{cases} 1, & \text{with probability } p, \\ 0, & \text{with probability } 1 - p, \end{cases} \quad (2)$$

and  $a_i^\dagger$  and  $a_j$  are electron creation and annihilation operators.

Quantum percolation exhibits a MIT as  $p$  is increased from zero, at least for three dimensions and above.<sup>7-9</sup> In two dimensions, some studies indicate a transition,<sup>10-14</sup> while others do not.<sup>15,16</sup> Analytical work on the Bethe lattice indicates that the quantum percolation transition may be in the same universality class as geometric percolation.<sup>17,18</sup> However,

the transition probability  $p_q$ , above which there exist extended zero-energy wave functions is greater than the threshold above which there exists a spanning cluster,  $p_c$ .<sup>17,18</sup> The geometric percolation transition is continuous and therefore, presumably, so is the quantum percolation transition.

Recently, we have studied quantum  $k$ -core percolation on the Bethe lattice.<sup>4</sup> The term  $k$  core refers to a geometrical constraint where every occupied bond must have at least  $k - 1$  occupied neighboring bonds.<sup>19-24</sup> To enforce this constraint, bonds are initially occupied independently and at random with probability  $p$ . Then, those occupied bonds with less than  $k - 1$  occupied neighboring bonds are rendered unoccupied. This removal procedure continues recursively throughout the lattice until all occupied bonds satisfy the  $k$ -core constraint. See Fig. 1 for an example on the Bethe lattice with coordination number  $z$ . Classically, this geometric constraint may have implications for glassy systems,<sup>25</sup> jamming systems,<sup>23</sup> and even biological systems.<sup>26</sup> Here, we investigate how such a geometric constraint affects the quantum-mechanical wave function embedded in this random geometry. We present a possible experimental realization of this theoretical investigation in the discussion.

Given the newness of geometric (classical)  $k$ -core percolation, we review its features before addressing the quantum-mechanical version. For  $k \leq 2$ , the mean-field geometric percolation transition is continuous; however, for  $k \geq 3$ , the mean-field geometric percolation transition is discontinuous. More specifically, the fraction of occupied bonds in the spanning  $k$ -core cluster,  $P_\infty$ , scales with  $p$  as  $P_\infty = P_0 + P_1(p - p_c)^{1/2}$  for  $p \geq p_c$  (with  $p_c - p \ll 1$ ), where  $P_0$  and  $P_1$  are constants and  $p_c$  is the critical occupation probability for classical (geometric) percolation. Note that above the transition, the square-root scaling indicates a transition that differs from an ordinary discontinuous transition, i.e., first-order transition, where the scaling would be linear and the transition driven by nucleation. The  $k \geq 3$  mean-field percolation transition is a *random* first-order phase transition where there exists diverging length scales in addition to the

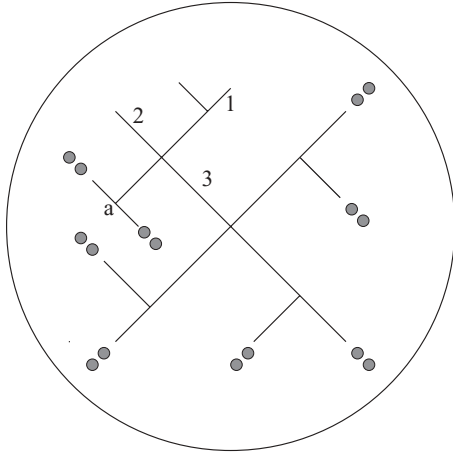


FIG. 1. Here  $k = 3$  and coordination number  $z = 4$ . Only occupied bonds are shown. The shaded circles denote branches that are  $k - 1$  connected to infinity. The removal of bonds 1 and 2 eventually triggers the removal of bond 3 and bonds emanating from vertex a, including the shaded circles. The remaining three branches emanating from the center site survive the removal process.

jump in the order parameter at the transition. For instance, the correlation length associated with the likelihood of two bonds some distance away from each other participating in the same spanning ( $k \geq 3$ )-core cluster diverges with a correlation length exponent of  $1/4$ . This correlation length exponent and the order parameter exponent of  $1/2$  (as well as other exponents) constitute a new universality class for a percolation transition.<sup>21,23</sup>

As for a quantum version of  $k$ -core percolation, once the geometric  $k$ -core constraint has been implemented, we then impose the usual quantum percolation property that electrons can only hop along occupied bonds. On the Bethe lattice, we can then compute the quantum conduction through the system self-consistently after assuming that the electronic wave function randomizes between bonds, i.e., the length scale of the disorder  $l_d$  is much greater than the coherence length  $l_c$ . Within this scheme, for  $k = 0, 1$ , the model reduces to ordinary quantum percolation, and we found that  $1 > p_q > p_c$ , where

$p_c$  signals the onset of the geometric percolation transition and  $p_q$  signals the onset of quantum conduction. We also found a random first-order transition for  $k > 2$  and that, interestingly enough, the critical threshold is the same as the  $k$ -core geometrical percolation critical point. This transition should be contrasted with the Anderson-type MIT, which yields a continuous transition (as does the ordinary quantum percolation transition on the Bethe lattice).

In this work, we numerically investigate the level statistics of quantum  $k$ -core percolation to compare with our previous analytical results on the Bethe lattice obtained in the limit  $l_d \gg l_c$ . In other words, how robust are our previous results in identifying a new universality class of disorder-driven MITs? Level statistics and its roots in random matrix theory are an important tool for studying universality, for example.<sup>27</sup> Correlations between energy eigenvalues of an individual quantum particle in a random potential in the conductive regime agree with results from Gaussian matrix ensembles.<sup>28</sup> In the localized regime, correlations between the energy eigenvalues are absent, and the level statistics become Poissonian. Right at the MIT, however, the level statistics are distinct from Gaussian matrix ensembles.<sup>29</sup> While these results pertain to the Anderson model where the disorder is on site, the same analysis has been applied to quantum percolation on a cubic lattice, where the disorder is off-diagonal, and similar results have been found.<sup>30</sup> In fact, the critical exponent for the divergence of the localization length extracted from the level statistics analysis is somewhat consistent with the Anderson model. Therefore, we will implement a similar numerical analysis for quantum  $k$ -core percolation on a Bethe-like lattice to go beyond our previous approximation.<sup>4</sup>

We, however, will not investigate the level statistics of quantum  $k$ -core percolation on finite-dimensional lattices for now. It turns out that  $k$ -core percolation on finite-dimensional lattices either exhibits properties of  $k = 0$  geometric percolation or no transition. See, for example, Ref. 31. One has to invoke more sophisticated constraints to observe different universal behavior from  $k = 0$  geometric percolation,<sup>32</sup> so we expect the quantum behavior to be similar to quantum percolation for finite-dimensional lattices, though this conjecture should ultimately be tested.

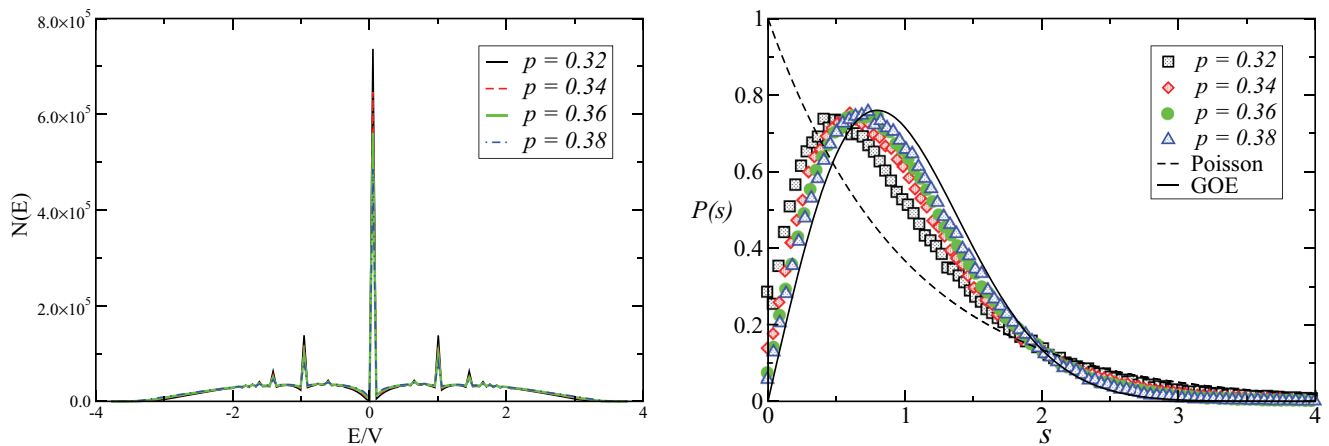


FIG. 2. (Color online) (left) The DOS for  $L = 15$  and different bond occupation probabilities. (right)  $P(s)$  for  $L = 15$  for different  $p$ s. The Wigner and Poisson forms are also shown.

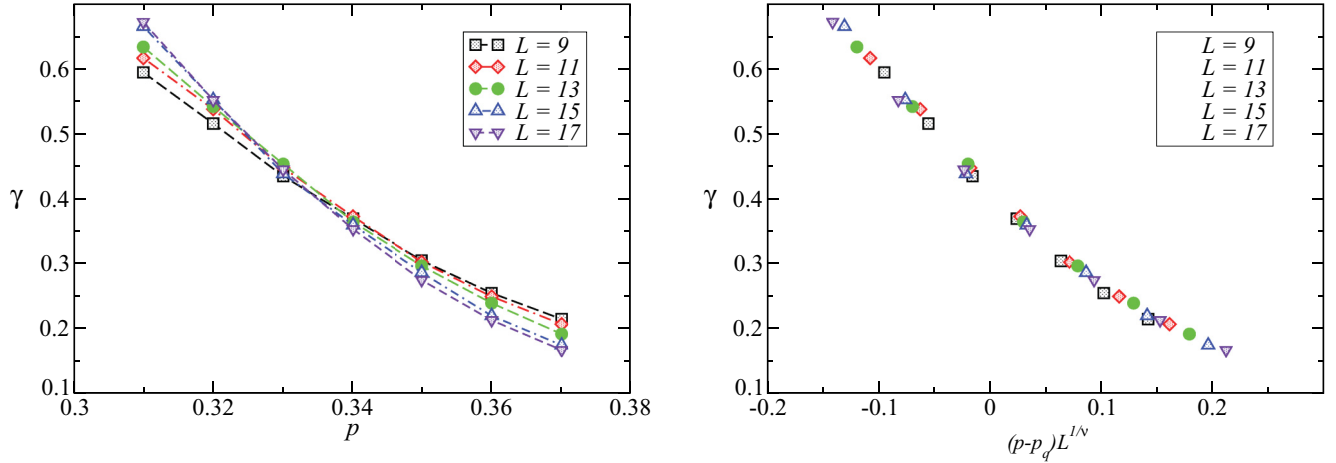


FIG. 3. (Color online) (left) The function  $\gamma(p, L)$  for different system sizes. (right) Scaling collapse for the cubic lattice.

This paper is organized as follows. We review the methodology and results for quantum percolation on the cubic lattice<sup>30</sup> as a means for calibration and then present our results for quantum ( $k = 0$ )-core percolation and quantum ( $k = 3$ )-core percolation on a Bethe-like lattice. We conclude with a discussion of the implications of our results, including a possible experimental realization.

## II. QUANTUM PERCOLATION ON THE CUBIC LATTICE

First, we analyze the level statistics for quantum percolation on the cubic lattice. To do so, we diagonalize the Hamiltonian defined by Eqs. (1) and (2) on the cubic lattice of length  $L$  with periodic boundary conditions to obtain a sequence of eigenvalues. This sequence is calculated for different realizations and increasing system sizes. The average density of states (DOS) for  $L = 15$  as a function of occupation probabilities is presented in Fig. 2. The sharp peaks are due to small disconnected structures, as discussed in Ref. 30. Now, one can apply the various measures of level statistics only if the density of states is smooth. There exists a smooth energy range around 0.4. The eigenenergies near this range are then arranged from highest to lowest, and the nearest-neighbor level spacing  $S$  is calculated and subsequently normalized by the average nearest-neighbor level spacing; i.e., normalized level spacing is denoted by  $s = S/\langle S \rangle$ .

One can then study the probability distribution for these level spacings,  $P(s)$ , as a function of  $p$  and  $L$ . When the system is in the insulator regime, the eigenfunctions are localized and therefore do not interact with each other such that  $P(s)$  is Poisson distributed, i.e.,  $P(s) = e^{-s}$ . When the system is in the metallic regime, Altshuler and Shklovskii<sup>28</sup> argued that if the width of the energy band of a sample  $E < E_c \equiv hD/L^2$ , where  $L^2/D$  is the characteristic time for an electron to diffuse through the sample, then the Hamiltonian of the system is characteristic of a Gaussian orthogonal ensemble (GOE) in the absence of a magnetic field or spin-orbit scattering. More specifically,  $P(s)$  obeys the Wigner-Dyson distribution,  $P(s) = \frac{\pi s}{2} \exp(-\frac{\pi}{4}s^2)$ . The cubic conductance,  $\langle G \rangle = \frac{e^2}{h} \langle N(E_c) \rangle = \frac{e^2}{h} \frac{E_c}{\langle S \rangle}$ , where  $N(E)$  is the number of levels in a band of width  $E$ . The conductance tends to infinity when

$L \rightarrow \infty$  in the metallic regime; thus  $E < E_c$  is satisfied, and the level spacing distribution obeys the Wigner-Dyson distribution for the GOE.

The plot of  $P(s)$  as a function of bond occupation probability for  $L = 15$  and an energy range of  $[0.2, 0.6]$  is displayed in Fig. 2. Figure 2 shows the expected transition from Wigner-like behavior for large  $p$  to Poisson behavior for small  $p$ . Note that all curves intersect at  $s \simeq 2$ , as observed in the Anderson model.<sup>29</sup> Other energy ranges studied yielded similar results. A convenient way to obtain the critical exponent  $\nu$ , characterizing the diverging localization length at the transition, is to study the parameter  $\gamma$ , defined as

$$\gamma = \frac{\int_2^\infty P(s) ds - e^{-\pi}}{e^{-2} - e^{-\pi}}, \quad (3)$$

which characterizes the transition from Wigner to Poisson as  $p$  is decreased. Note that  $\gamma$  should increase from 0 to 1, as  $P(s)$  goes from Wigner to Poisson. Denoting  $\xi(p)$  as the localization length [such that  $\xi(p) \sim (p - p_q)^{-\nu}$ ], the above parameter is expected to demonstrate scaling behavior,  $\gamma(p, L) = f[L/\xi(p)]$ . In the vicinity of the critical quantum bond probability  $p_q$ ,

$$\gamma(p, L) = \gamma(p_q) + C \left| \frac{p}{p_q} - 1 \right| L^{1/\nu}, \quad (4)$$

where  $C$  is a constant.

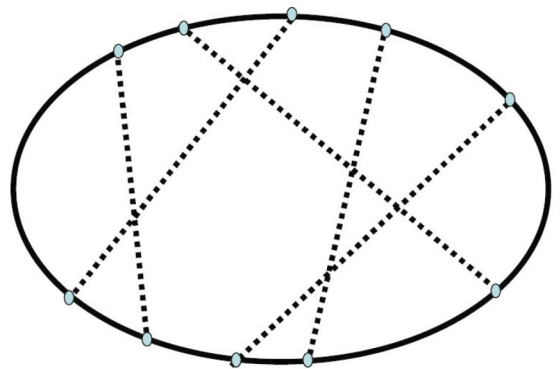


FIG. 4. (Color online) An example of a Bethe-like lattice with coordination number  $z = 3$ . Dotted curves indicate the random pairs.

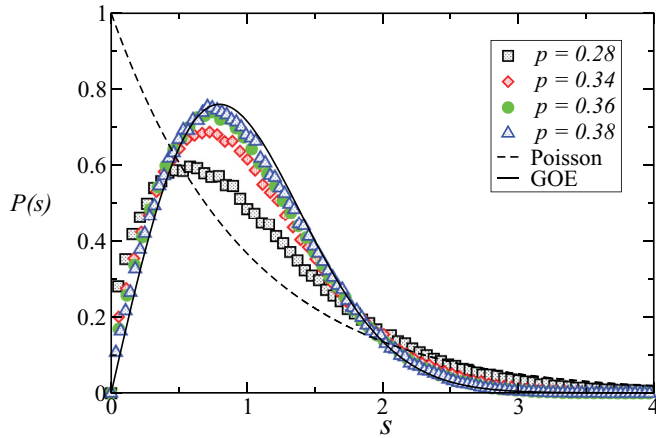


FIG. 5. (Color online)  $P(s)$  for the Bethe-like lattice for  $N = 1024$  and  $k = 0$  for different  $p$ .

Figure 3 plots  $\gamma$  as a function of  $p$  around  $p_q$  for increasing  $L$ . The curves intersect near a single point given by  $p_q \cong 0.334$ . This result is consistent with the result in Ref. 30. The single crossing point indicates that there exists a metal-insulator transition and one can apply the scaling collapse suggested above. The optimal scaling collapse shown in Fig. 3 yields  $\nu = 1.60 \pm 0.05$ , which should be compared to  $1.32 \pm 0.08$  obtained in Ref. 30. Our latest result is even closer to the Anderson result than the previous work, where the most precise measurement is  $\nu = 1.58 \pm 0.02$ .<sup>33</sup>

### III. QUANTUM $k$ -CORE PERCOLATION ON A BETHE-LIKE LATTICE

To test our analytical results for quantum  $k$ -core conduction on the Bethe lattice, a connected, loop-free graph with a fixed coordination number, one should perform simulations on the Bethe lattice. However, the surface effects on finite-size lattices dominate over bulk effects, making the numerical results difficult to interpret. So, following the procedure presented in Ref. 34, we construct a Bethe-like lattice by first considering a one-dimensional ring with  $N$  sites such that each lattice site has two bonds emanating from it. Next, additional bonds

are constructed between different lattice sites at random. The number of random pairs connecting different lattice sites depends on the fixed coordination number  $z$ . More specifically, there must be  $z$  bonds per site. See Fig. 4 for an example with  $z = 3$ . As  $N$  increases, the average number of loops of length  $l$  increases as  $(z - 1)^l$ , such that the fraction of all lattice sites belonging to any loop of length  $\leq l$  for  $l \ll \ln(N)/\ln(z - 1)$  is negligible. Therefore, the structure becomes increasingly treelike as  $N$  increases. Moreover, the lack of a surface makes the numerical interpretation of measurements performed on this structure easier. We should also point out that this Bethe-like lattice shares similar properties with random regular graphs.<sup>35</sup>

#### A. $k = 0$

For  $k = 0$ , Harris<sup>18</sup> gave a theoretical prediction of  $p_q$  on the Bethe lattice. One must simply solve  $1 + (p_q \sigma^2)^{-1} = (p_q \sigma)^{2/(\sigma-1)}$ , with  $\sigma = z - 1$ . By solving Harris's self-consistency equation above for  $z = 6$ ,  $p_q = 0.265$ . We can test this result numerically with the level statistics analysis. Figure 5 plots  $P(s)$  for different  $p$ s with  $N = 1024$ ,  $z = 6$ , and an energy range of  $[0.3, 0.8]$ . Figure 6 plots  $\gamma(p, N)$  for  $z = 6$ . The curves intersect near  $p \sim 0.3$ , which is close to the analytical result for the Bethe lattice, though the agreement is not precise. The difference between the analytical calculation and our numerical calculation is presumably due to the nature of the lattice such that the quantum mechanics is much more sensitive to loops than geometric percolation. To test this notion, when measuring the onset of geometric percolation on the Bethe-like lattice, we do arrive at good agreement between the analytical result,  $p_c = 1/(z - 1)$ , and our numerical result.

Moreover, the crossing point in Figure 6 indicates that we can collapse the data by assuming that, instead of  $\gamma(p, L) = f[L/\xi(p)]$  in the cubic lattice case, now  $\gamma(p, N) = f[N/N^*(p)]$ , where  $N^*$  is a crossover size similar to the localization length in the three-dimensional case. In other words,  $N^* \sim (p - p_q)^{-\nu'}$ . Therefore,  $\gamma(p, N) = f[N^{1/\nu'}(p - p_q)]$ . It has been conjectured that  $\nu' = d_u \nu_{MF}$ , where  $d_u$  is the upper critical dimension and  $\nu_{MF}$  is the mean-field correlation length exponent.<sup>36</sup> For geometric percolation,  $d_u = 6$  and

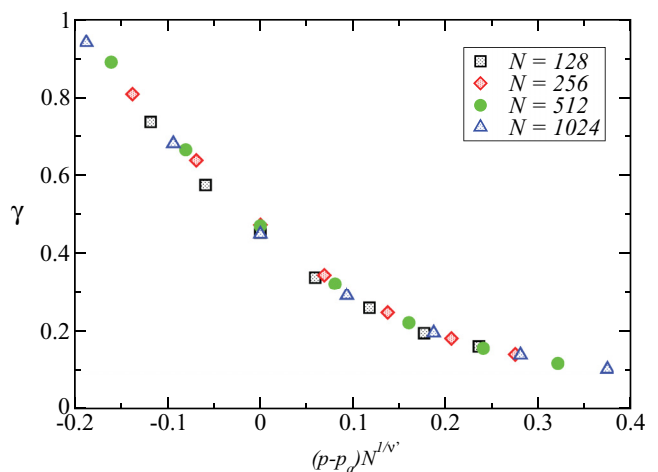
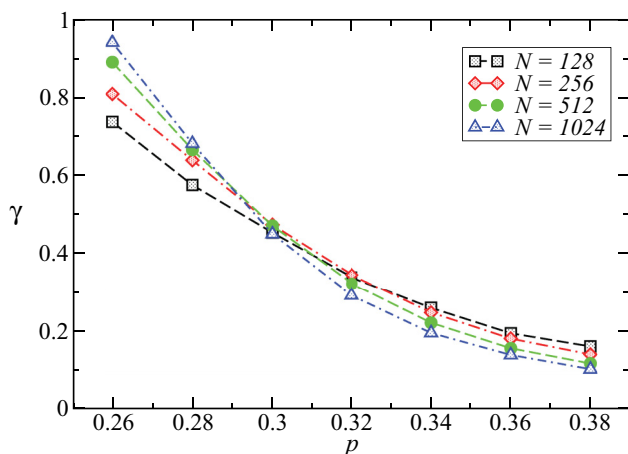


FIG. 6. (Color online) (left) The function  $\gamma(p)$  for different system sizes. (right) The scaling collapse for  $\gamma(p)$ .

$\nu_{MF} = 1/2$ , such that  $\nu' = 3$ . To date, the upper critical dimension of quantum percolation is not known. Interestingly, the upper critical dimension for the Anderson model is potentially infinite, such that the mean-field correlation length exponent scales with dimension  $d$ .<sup>37</sup> More precisely,  $\nu = \frac{1}{2} + \frac{1}{d-2}$ .

Figure 6 shows the optimal scaling collapse to yield the exponent  $\nu' = 4.5 \pm 0.2$ , assuming that  $p_q = 0.300(1)$ . If we assume  $p_q = 0.265$ , then we do not arrive at a good scaling collapse. Regarding  $\nu'$ , if we assume the same mean-field correlation length exponent of  $\nu_{MF} = 1/2$  as in classical  $k = 0$  percolation, which is consistent with the previous work of Harris<sup>18</sup> showing that the mean-field susceptibility for zero-energy eigenstates diverges with the same exponent as in the geometric percolation problem (with  $p_q$  replacing  $p_c$ ), then we extract an upper critical dimension of  $d_u = 9$ . If, on the other hand, the upper critical dimension is infinite, as in the case of the Anderson model, then a different analysis must be undertaken.

### B. $k = 3$

In Ref. 4, we gave an example of a MIT driven by ( $k = 3$ )-core disorder on the Bethe lattice with  $z = 4$ . More precisely, the quantum conduction as a function of occupation probability  $p$  is a random first-order transition with  $p_q = p_c$ . In other words, the quantum conduction jumps discontinuously from zero at the transition and then increases with  $(p - p_q)^{1/2}$ . To obtain this result, we assumed that the phase randomizes between levels on the Bethe lattice, i.e.,  $l_d \gg l_c$ . Here, we use level statistics to test the robustness of our prior results. Since the geometric critical percolation occupation probability  $p_c$  is  $8/9$ , which is close to 1, we choose  $z = 6, k = 3$ , whose  $p_c = 0.603$ .<sup>19,22,23</sup>

We first tested this analytical result on the Bethe-like lattice. Recall that to implement the geometric  $k$ -core constraint, one first occupies the bonds at random and independently and then begins the  $k$ -core culling procedure where bonds that do not obey the  $k$ -core constraint are recursively culled until all bonds obey the  $k$ -core constraint. With this culling process, some samples may end up with no occupied bonds. Moreover,

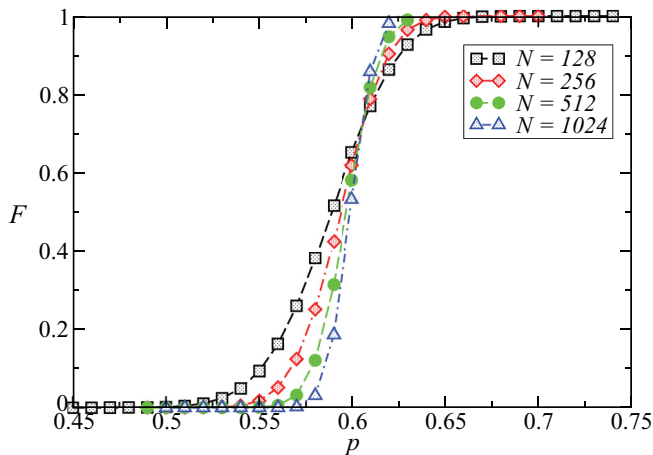


FIG. 7. (Color online) Fraction of remaining samples after applying the  $k$ -core removal/culling procedure,  $F$ , vs occupation probability on the Bethe-like lattice for  $z = 6, k = 3$ .

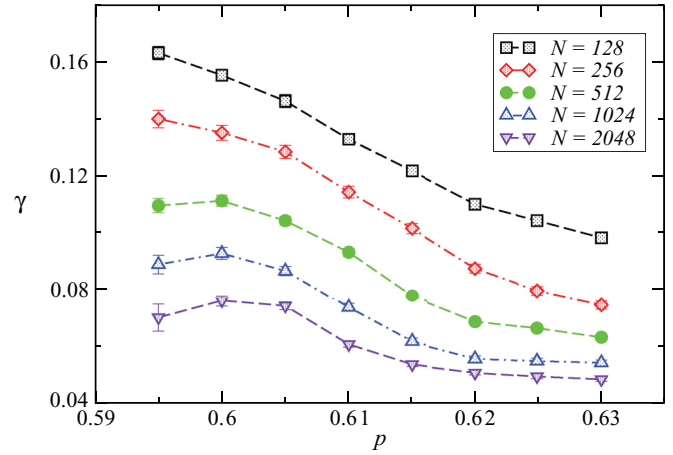


FIG. 8. (Color online)  $\gamma$  as a function of  $p$  for different system sizes for the  $z = 6, k = 3$  Bethe-like lattice.

for  $k = 3$  on the Bethe lattice, any samples with remaining occupied bonds must form a spanning cluster. Therefore, if we record the fraction of samples with occupied bonds after the culling procedure, this approximates the probability of spanning (since we are working with a Bethe-like lattice). Figure 7 depicts the fraction of the remaining samples after the  $k$ -core culling procedure, denoted by  $F$ , versus occupation probability for  $z = 6, k = 3$ , and different system sizes. There exists a well-defined crossing point such that in the infinite system limit, all occupied bonds are removed due to the  $k$ -core constraint for  $p < 0.604$ , while for  $p > 0.604$ , occupied bonds remain. Note that  $p_c = 0.604$  is quite close to the analytical  $p_c$  for  $z = 6$  and  $k = 3$  for the classical problem.

Now we address the quantum results. Figure 8 plots  $\gamma$  as a function of  $p$  for different system sizes. With no remaining occupied bonds for  $p < p_c$ , the system is insulating in a trivial sense and not in the sense that  $\gamma \rightarrow 1$ . We observe that  $\gamma$  decreases with increasing system size, as expected. Moreover, the increasing size of the error bar with increasing system size indicates less remaining occupied samples due to the  $k$ -core constraint. What happens for  $p > p_c$ ? The data indicate that  $\gamma$  tends to 0 as the system size increases for  $p > p_c$ , indicating that it is a metallic system. There is no crossing point above  $p_c$  such that  $p_c$  must equal  $p_q$  as was obtained previously. Note that we could have observed a crossing point somewhere above  $p_c$  to indicate that  $p_q > p_c$ , but we do not. The data imply a discontinuous transition since  $\gamma$  tends towards zero as  $N$  becomes large for  $p \geq p_c = p_q$ .

## IV. DISCUSSION

We have analyzed the level statistics for quantum  $k$ -core percolation. Our results for  $k = 0$  core on the cubic lattice are consistent with previous results from Ref. 30. For quantum ( $k = 0$ )-core percolation on a Bethe-like lattice, by measuring  $\gamma(p)$ , a parameter that defines how the level statistics go from Poissonian to Wigner as the system becomes metallic, we find a threshold probability that differs somewhat from Harris's Bethe lattice result.<sup>18</sup> This difference is due to the sensitivity of quantum mechanics to loops occurring in the Bethe-like lattice and warrants further investigation. Moreover, our result

is presumably the first numerical test of a closed-form result for quantum ( $k = 0$ )-core percolation. In addition, for quantum ( $k = 0$ )-core percolation on a Bethe-like lattice, a scaling collapse of  $\gamma(p)$  with varying system sizes yields a new quantum critical exponent,  $\nu' = 4.5(2) = \nu_{MF}d_u$ . Assuming the correlation length exponent is the same as the mean-field result for geometric percolation, which is consistent with the Harris calculation,<sup>18</sup> the upper critical dimension is  $d_u = 9$ . On the other hand, this new quantum critical exponent differs from the geometric one where  $\nu'_g = 3$ , again demonstrating the quantum sensitivity to loops.

We have also demonstrated the robustness of our previous work for quantum ( $k = 3$ )-core percolation on the Bethe lattice where we found a random first-order MIT.<sup>4</sup> In going beyond the random-phase approximation made in Ref. 4, the level statistics on the Bethe-like lattice shows  $p_q = p_c$ , as before. In fact, for  $p < p_c$ , all bonds are removed, and the system is trivially an insulator. For  $p \geq p_c$ , the data suggest that the system immediately goes to the Wigner-Dyson regime without going through a different regime at the transition, indicating a discontinuous transition, which also agrees with our previous work.<sup>4</sup>

Therefore, our work provides an important counterexample for the Mott versus Anderson MIT paradigm, where disorder-driven (Anderson) MITs are continuous and interaction-driven (Mott-Hubbard) MITs are discontinuous. Our counterexample is due to the correlations in the disorder as a result of the  $k$ -core constraint. Correlations in the disorder have been shown previously to “complicate” matters. For instance, in one-dimensional wires with long-range, correlated disorder, there exists a MIT that does not happen in the short-range, uncorrelated disorder case.<sup>38</sup> Of course, the quantum ( $k = 3$ )-core percolation transition is not a typical discontinuous transition, as indicated in Ref. 4, where the quantum conduction increases as  $(p - p_q)^{1/2}$  beyond the transition. We expect to

find a diverging correlation length in the quantum conduction, though more work needs to be done to confirm this.

As for experimental implications, there are many experiments in the realm of classical transport on ordinary percolating systems. See, for example, Ref. 39 for a recent one on nanowire composites. In addition, transport in undoped graphene is linked to classical electronic transport on percolating networks, though quantum effects are also relevant.<sup>40</sup> However, can a quantum ( $k = 3$ )-core percolation transition ever be realized? An experiment has already been conducted with a two-dimensional collection of silver quantum dots sitting on top of a Langmuir monolayer at room temperature.<sup>41</sup> As the interparticle spacing decreases by compressing the floating particles together, the electronic transport goes from hopping to tunneling to ordinary metallic transport. The authors argue that disorder in the particle size and in the charging energy probably does not drive the transition and, instead, conjecture a possible first-order Mott transition at *room temperature*. However, in light of the analysis of the onset of classical conduction for a  $k = 3$  core, where  $k$  encodes the scalar aspect of local mechanical stability in particle packings,<sup>23</sup> we argue for a possible *classical* ( $k = 3$ )-core percolation transition in conduction. A quantum analog of this experiment can potentially be realized in low-temperature packings of metallic nanoparticles such that at least three particles are needed for mechanical stability as encoded by the ( $k = 3$ )-core constraint. Such an experiment would allow one to search for this new universality class of quantum disorder-driven MITs.

## ACKNOWLEDGMENTS

J.M.S. gratefully acknowledges funding support from Grant No. NSF-DMR-CAREER-0645373.

<sup>1</sup>N. F. Mott, *Rev. Mod. Phys.* **40**, 677 (1968).

<sup>2</sup>P. W. Anderson, *Phys. Rev.* **109**, 1492 (1958).

<sup>3</sup>F. Evers and A. D. Mirlin, *Rev. Mod. Phys.* **80**, 1355 (2008).

<sup>4</sup>L. Cao and J. M. Schwarz, *Phys. Rev. B* **82**, 104211 (2010).

<sup>5</sup>P. G. de Gennes, P. Lafore, and J. P. Millot, *J. Phys. Chem. Solids* **11**, 105 (1959).

<sup>6</sup>G. Schubert and H. Fehske, in *Quantum and Semi-classical Percolation and Breakdown in Disordered Solids*, Lecture Notes in Physics Vol. 762 (Springer, Berlin, 2009), p. 135.

<sup>7</sup>G. Schubert, A. Weiße, and H. Fehske, *Phys. Rev. B* **71**, 045126 (2005).

<sup>8</sup>I. Travenec, *Int. J. Mod. Phys. B* **22**, 5217 (2008).

<sup>9</sup>A. Kaneko and T. Ohtsuki, *J. Phys. Soc. Jpn.* **68**, 1488 (1999).

<sup>10</sup>Y. Meir, A. Aharony, and A. B. Harris, *Europhys. Lett.* **10**, 275 (1989).

<sup>11</sup>D. Daboul, I. Chang, and A. Aharony, *Eur. Phys. J. B* **16**, 303 (2000).

<sup>12</sup>M. F. Islam and H. Nakanishi, *Phys. Rev. E* **77**, 061109 (2008).

<sup>13</sup>H. Nakanishi and M. F. Islam, in *Quantum and Semi-classical Percolation and Breakdown in Disordered Solids*, Lecture Notes in Physics Vol. 762 (Springer, Berlin, 2009), p. 109.

<sup>14</sup>G. Schubert and H. Fehske, *Phys. Rev. B* **77**, 245130 (2008).

<sup>15</sup>C. M. Soukoulis and G. S. Grest, *Phys. Rev. B* **44**, 4685 (1991).

<sup>16</sup>A. Mookerjee, I. Dasgupta, and T. Saha, *Int. J. Mod. Phys. B* **9**, 2989 (1995).

<sup>17</sup>A. B. Harris, *Phys. Rev. Lett.* **49**, 296 (1982).

<sup>18</sup>A. B. Harris, *Phys. Rev. B* **29**, 2519 (1984).

<sup>19</sup>J. Chalupa, P. L. Leath, and G. R. Reich, *J. Phys. C* **12**, L31 (1979).

<sup>20</sup>B. Pittel, J. Spencer, and N. Wormald, *J. Comb. Theory, Ser. B* **67**, 111 (1996).

<sup>21</sup>S. N. Dorogovtsev, A. V. Goltsev, and J. F. F. Mendes, *Phys. Rev. Lett.* **96**, 040601 (2006).

<sup>22</sup>A. V. Goltsev, S. N. Dorogovtsev, and J. F. F. Mendes, *Phys. Rev. E* **73**, 056101 (2006).

<sup>23</sup>J. M. Schwarz, A. J. Liu, and L. Q. Chayes, *Europhys. Lett.* **73**, 560 (2006).

<sup>24</sup>A. B. Harris and J. M. Schwarz, *Phys. Rev. E* **72**, 046123 (2005).

<sup>25</sup>M. Selitto, C. Toninelli, and G. Biroli, *Europhys. Lett.* **69**, 496 (2005).

<sup>26</sup>D. J. Schwab, R. F. Bruinsma, J. L. Feldman, and A. J. Levine, *Phys. Rev. E* **82**, 051911 (2010).

- <sup>27</sup>M. L. Mehta, *Random Matrices* (Academic, San Diego, 1991), and the references therein.
- <sup>28</sup>B. L. Altshuler and B. I. Shklovskii, *Zh. Eksp. Teor. Fiz.* **91**, 220 (1986) [*Sov. Phys. JETP* **64**, 127 (1986)].
- <sup>29</sup>B. I. Shklovskii, B. Shapiro, B. R. Sears, P. Lambrianides, and H. B. Shore, *Phys. Rev. B* **47**, 11487 (1993).
- <sup>30</sup>R. Berkovits and Y. Avishai, *Phys. Rev. B* **53**, R16125 (1996).
- <sup>31</sup>M. C. Medeiros and C. M. Chaves, *Phys. A* **234**, 604 (1997); C. M. Chaves and B. Koiller, *ibid.* **218**, 271 (1995).
- <sup>32</sup>M. Jeng and J. M. Schwarz, *Phys. Rev. E* **81**, 011134 (2010).
- <sup>33</sup>K. Slevin and T. Ohtsuki, *Phys. Rev. Lett.* **82**, 382 (1999).
- <sup>34</sup>D. Dhar, P. Shukla, and J. P. Sethna, *J. Phys. A* **30**, 5259 (1997).
- <sup>35</sup>See, for example, O. Melchert, A. K. Hartmann, and M. Mezard, *Phys. Rev. E* **84**, 041106 (2011).
- <sup>36</sup>Y. Kim, Y. Ko, and S. H. Yook, *Phys. Rev. E* **81**, 011139 (2010).
- <sup>37</sup>A. M. Garcia-Garcia, *Phys. Rev. Lett.* **100**, 076404 (2008).
- <sup>38</sup>P. Carpena, P. Benaola, P. C. Ivanov, and H. E. Stanley, *Nature (London)* **418**, 955 (2002).
- <sup>39</sup>S. I. White, R. M. Mutiso, P. M. Vora, D. Jahnke, S. Hsu, J. M. Kikkawa, J. Li, J. E. Fischer, and K. I. Winey, *Adv. Funct. Mater.* **20**, 2709 (2010).
- <sup>40</sup>V. V. Cheianov, V. I. Fal'ko, B. L. Altshuler, and I. L. Aleiner, *Phys. Rev. Lett.* **99**, 176801 (2007).
- <sup>41</sup>G. Markovich, C. P. Collier, and J. R. Heath, *Phys. Rev. Lett.* **80**, 3807 (1998).